The Relationship Between Initiation of Landslides and Rainfall Intensity-Duration Thresholds in South-East Queensland, Australia

Chaminda Gallage * , Tharindu Abeykoon , Jessica Trofimovs

Posted Date: 13 April 2026

doi: 10.20944/preprints202604.0798.v1

Keywords: rainfall thresholds; rainfall-induced landslides; slope stability; rainfall data; statistical analysis

 doi:10.20944/preprints202604.0798.v1

Article

The Relationship Between Initiation of Landslides and Rainfall Intensity-Duration Thresholds in South-East Queensland, Australia

Chaminda Gallage [1,*], Tharindu Abeykoon [1] and Jessica Trofimovs [2]

[1] School of Civil and Environmental Engineering, Science and Engineering Faculty, Queensland University of Technology, Brisbane 4000, Queensland, Australia

[2] School of Earth and Atmospheric Sciences, Faculty of Science, Queensland University of Technology, Brisbane 4000, Queensland, Australia

* Correspondence: chaminda.gallage@qut.edu.au

Abstract

Rainfall attributes to slope instability by increasing soil moisture, reducing soil's matric suction and elevating pore water pressure. As such, rainfall thresholds are often used to predict the likelihood of slope failures by establishing the minimum rainfall conditions or parameters necessary to initiate a landslide. However, the reliability and accuracy of thresholds need to be rigorously validated prior to adopting them in operational warning systems. This study aims to develop empirical rainfall thresholds for the initiation of shallow landslides in South-East Queensland (SEQ), Australia, where rainfall-induced sediment-related disasters occur annually. The current study examines 104 rainfall-induced shallow landslides that occurred during 1974-2018. The corresponding rainfall conditions were analysed objectively from rainfall data to derive the thresholds using the quantile regression method, separating rainfall events by the absence of rainfall for 24 h. The thresholds were determined for the different quantiles (i.e., 2nd, 10th, 50th and 90th), and the 2nd percentile quantile was considered the rainfall threshold for SEQ. In order to render comparable rainfall thresholds for various regions with normalised rainfall intensity, the study also proposed I_{MAP}-D thresholds for SEQ, in terms of mean annual precipitation (MAP). Further, the developed I-D threshold is validated using the physical-based real-time monitoring system at Maleny, Queensland, Australia. The validation provides an optimal balance between the maximisation of accurate predictions and the minimisation of inaccurate predictions, fostering the operational use of validated rainfall thresholds in the operational early warning system for regional shallow landslide forecasting.

Keywords: rainfall thresholds; rainfall-induced landslides; slope stability; rainfall data; statistical analysis

1. Introduction

Rainfall is a primary triggering factor for slope instabilities, acting to increase soil moisture, reduce matric suction, and elevate pore water pressure. Exploiting this hydro-geomechanical relationship, rainfall thresholds form the foundation of most existing landslide early warning systems designed to predict potential slope failures [1–3]. These thresholds are derived by analysing historical meteorological events to define empirical or statistical correlations between rainfall characteristics and localised landslide occurrences. This correlation is typically expressed as a deterministic mathematical function, operating on the fundamental assumption that past relationships between precipitation metrics and slope failure initiation remain valid for predicting future events. A significantly heightened probability of slope failure exists when contemporary rainfall events exceed these defined thresholds.

 doi:10.20944/preprints202604.0798.v1

The majority of empirical approaches to landslide monitoring rely on the statistical evaluation of past rainfall conditions that triggered instability [4]. The geomechanical rationale underlying this approach is that the groundwater conditions responsible for failure, such as the transient loss of apparent cohesion are intrinsically linked to infiltration rates, antecedent moisture content, rainfall history, and site-specific soil characteristics [5]. Consequently, these studies aim to formulate mathematical boundaries that represent the minimum rainfall conditions known to have triggered historical landslides [6]. In this context, a rainfall threshold defines the lower boundary of precipitation below which slope failure is assumed not to initiate. Unlike typical thresholds that feature both minimum and maximum boundaries, defining an upper threshold for rainfall-induced landslides is impractical, as slope failure can occur at any extreme above the minimum limit.

Despite extensive global research into rainfall thresholds for landslide initiation, there remains a notable gap in the Australian context, with the exception of a recent regional study focused on northern New South Wales (NSW) [7]. Addressing this critical gap, the current study establishes specific rainfall thresholds for South-East Queensland (SEQ). SEQ is highly susceptible to rainfall-induced landslides, receiving approximately 1050 mm of mean annual rainfall, heavily weighted by 415 mm of reliable summer precipitation (December to February). This seasonal concentration of extreme rainfall frequently leads to slope failures. Notably, severe torrential rains during the 2010–2011 summer resulted in widespread landslides, leading to the declaration of much of the state as a disaster zone [8].

Developing predictive capabilities for SEQ is therefore of high socioeconomic importance. However, the complex interactions between rainfall characteristics and slope conditions in this region require further study to confidently establish robust thresholds. This research determines regional intensity-duration (I-D) thresholds, antecedent thresholds, and normalised thresholds utilising a database of 104 historical landslide events recorded across SEQ between 1974 and 2018.

Rainfall intensity-duration (I-D) thresholds are the most prevalent metric used in the literature [9,10], generally taking the mathematical form:

$$I = c + \alpha D^{\beta} \quad (1)$$

Where I is the mean rainfall intensity, D is the rainfall duration, and $c \geq 0$, α, and β are empirical parameters. In this study, the parameters were calibrated over a duration range of 0.3 to 383 h, and intensities ranging from 0.1 to 36 mm/h. Aligning with standard methodologies, c = 0 was adopted, reducing the relationship to a simple power law ($I = \alpha D^{\beta}$). Global parameter reviews typically find β ranging between -2.00 and -0.19, and α ranging from 4.00 to 176.40 [5].

A primary limitation of strictly localised regional thresholds is their non-transferability to neighboring geographical areas due to variations in lithology, geomorphology, and climatic variability [11,12]. To mitigate this limitation and facilitate regional comparisons, normalisation of the rainfall intensity by the mean annual precipitation (MAP) is frequently applied [13]. Accordingly, this study develops I_{MAP}-D thresholds for SEQ. Literature indicates that these normalised thresholds also follow power laws, with the scaling exponent β generally falling between -0.79 and -0.21, and α ranging from 0.02 to 4.62 [5].

2. Study Area

The area of investigation is the South-East region of Queensland (SEQ). SEQ comprises eleven local government areas, including the City of Brisbane, City of Gold Coast, Sunshine Coast Region, Moreton Bay Region, Logan City, City of Toowoomba, City of Ipswich, and the recently de-amalgamated Shire of Noosa [14]. As the most urbanised region in the state, SEQ spans over 35,000 km^2 (extending 240 km north-south and 140 km east-west) and supports a population exceeding 3.6 million, accounting for approximately 75% of Queensland's total population. Demographic concentration makes the hazard of rainfall-induced slope failure highly significant. The spatial distribution of the local government areas within the study zone is illustrated in Figure 1.

 doi:10.20944/preprints202604.0798.v1

Figure 1. Study area - SEQ region.

3. Data Collection

3.1. Landslide Data

Historical landslide records spanning 1842 to 2018 were extracted from the Geoscience Australia database, which initially cataloged 1,974 national events. The database details event causes, impacts, dates, locations, and source references. Following the discontinuation of updates to this database in 2018, 156 landslide events were identified within the SEQ boundaries. After a rigorous filtering process to exclude events lacking temporally and spatially correlated rainfall data from proximate weather stations, the dataset was refined to 104 well-documented events. The geographical distribution of these landslides and the associated weather stations is plotted on Figure 2.

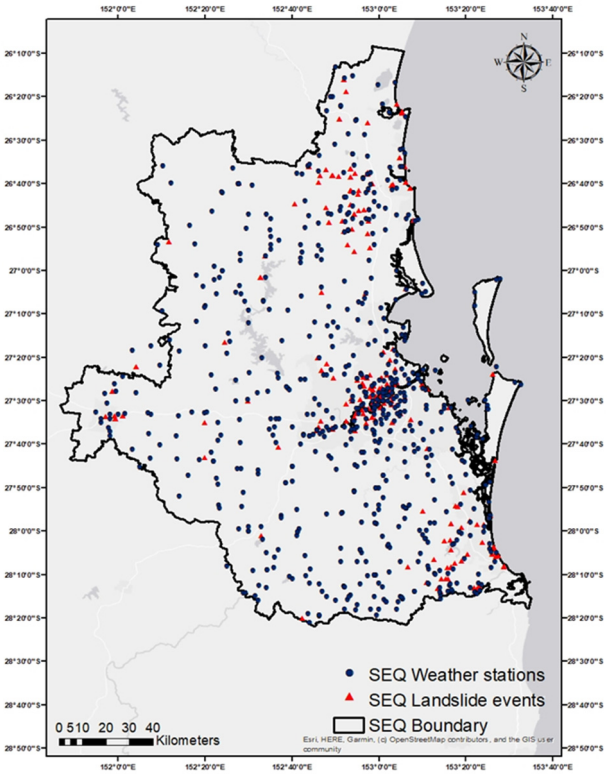

 doi:10.20944/preprints202604.0798.v1

Figure 2. Map of SEQ landslide event locations.

SEQ's topography, visually represented in the digital elevation model (DEM) in Figure 3, features steep, geomorphologically active terrains that, combined with the intensive summer rainfall regime, create highly conducive conditions for shallow slope failures.

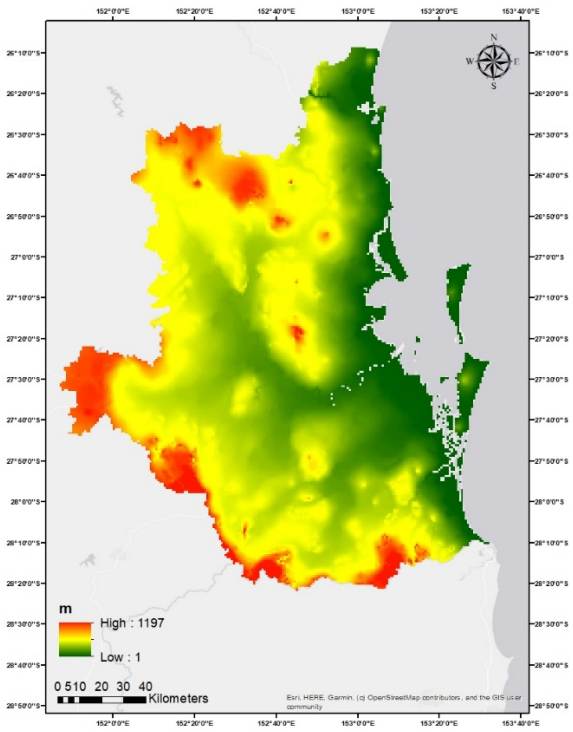

Figure 3. DEM of Australia (Elevations are in meters).

3.2. Rainfall Data

Rainfall datasets were sourced from the Australian Bureau of Meteorology (BOM), utilising continuous pluviographic data (6-minute intervals) alongside half-hourly and minutely recordings. Spatial correlation between landslide coordinates and BOM stations was executed using a Geographic Information System (GIS) framework. The spatial proximity was calculated using the Haversine formula, which computes the great-circle distance between two coordinate pairs on a sphere. While the Haversine method assumes a perfectly spherical earth (mean radius R = 6371 km) and neglects ellipsoidal effects and topographic elevation changes, previous validations confirm its accuracy for these specific spatial applications [15,16].

The mathematical operations applied are defined as follows:

$$\Delta lat = lat2 - lat1 \tag{2}$$

$$\Delta long = long2 - long1 \tag{3}$$

$$a = sin^2\left(\frac{\Delta lat}{2}\right) + \cos(lat1).\cos(lat2).sin^2\left(\frac{\Delta long}{2}\right) \tag{4}$$

$$c = 2atan^2\left(\sqrt{a}.\sqrt{1-a}\right) \tag{5}$$

$$d = R.c \tag{6}$$

Where lat1, long1, lat2, long2 are the latitude and longitude coordinates of two points of interest.

A custom MATLAB script processed over 23 million distance calculations to identify the optimal meteorological matches. A temporal logical function ensured the weather station was operational

 doi:10.20944/preprints202604.0798.v1

during the landslide event. The selection protocol dictated that the closest station within a 5 km radius was prioritised. In the absence of a station within 5 km, data from the three nearest stations within a 10 km radius were interpolated using the Inverse Distance Weighting (IDW) method [17]:

$$z_p = \frac{\sum_{i=1}^{n} \left(\frac{z_i}{d_i{}^p}\right)}{\sum_{i=1}^{n} \left(\frac{1}{d_i{}^p}\right)} \quad (7)$$

Where Z_p is the interpolated rainfall intensity/duration at the landslide location, Z_i represents the measured values at the proximal stations, d_i represents the respective distances, and p is the power parameter (set to 2 to heavily weight immediate proximity). Events lacking stations within the 10 km tolerance were discarded to maintain data integrity.

4. Determination of Rainfall I-D Thresholds for SEQ

A defined rainfall event was bounded by a minimum 24-hour non-rainfall antecedent period. Average intensity (I, in mm/h) and total duration (D, in hours) preceding the landslide initiation were derived for the refined dataset. The threshold boundary was mathematically constrained using quantile regression taking the form $\log I = \log \alpha + \beta \log D$ [2,5,9].

Quantile regressions for the 2nd, 10th, 50th, and 90th percentiles were established. Following recognised standards for conservative early warning systems, the 2nd percentile was adopted as the absolute minimum I-D threshold for SEQ [4,5]. Normalised I_{MAP}-D thresholds were determined similarly by rescaling the average intensity ($I_{MAP} = I / MAP$).

Quantile regression was explicitly selected over standard ordinary least squares (OLS) linear regression due to its robustness against outliers, non-uniform variance, and historical data anomalies [10,18]. By establishing the conditional median (or other quantiles) rather than the conditional mean [19], it provides a highly reliable mathematical lower-bound boundary necessary for risk thresholding. Data processing and curve fitting were executed using the quantreg package in RStudio [18].

5. Results

The analysed rainfall parameters initiating shallow landslides in SEQ, alongside the corresponding quantile regression curves plotted on double logarithmic axes, are presented in Figure 4. The dataset captures diverse meteorological conditions, with initiating intensities ranging from 0.15 mm/h to 13.7 mm/h, and event durations stretching from 0.3 h to 383 h.

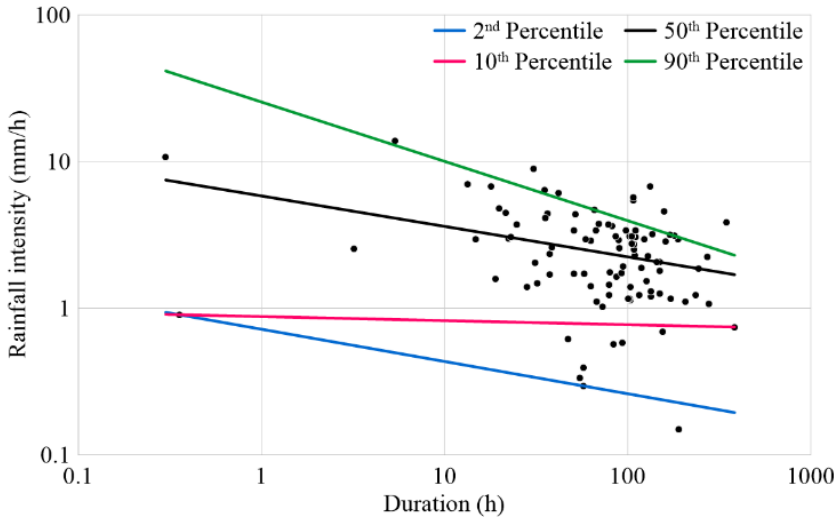

 doi:10.20944/preprints202604.0798.v1

Figure 4. Rainfall I-D conditions for shallow landslides in SEQ and the quantile regression lines for 2nd, 10th, 50th and 90th percentiles.

The thresholds obtained for SEQ are summarised in Tables 1 and 2 below, presenting the equations of the 2nd,10th, 50th, and 90th percentile regression lines, determined from the quantile regression using R-studio 'quantreg' analysis.

Table 1. Linearised rainfall I-D conditions for landslides initiation in SEQ.

Quantile	I-D threshold equation
2nd	$\log I = -0.22001 \log D + (-0.14303)$
10th	$\log I = -0.02771 \log D + (-0.05657)$
50th	$\log I = -0.20771 \log D + (0.76586)$
90th	$\log I = -0.40462 \log D + (1.40638)$

Table 2. Rainfall I-D conditions for landslides initiation in SEQ.

Quantile	I-D threshold equation	Duration range (h)
2nd	$I = 0.719 \times D^{-0.220}$	0.3 ≤D ≤383
10th	$I = 0.878 \times D^{-0.028}$	0.3 ≤D ≤383
50th	$I = 5.832 \times D^{-0.208}$	0.3 ≤D ≤383
90th	$I = 25.490 \times D^{-0.405}$	0.3 ≤D ≤383

The 50th percentile highlights the median geomechanical response of the region: as storm duration extends, the necessary intensity required to trigger instability reduces proportionally. Critically, the 2nd percentile (the early warning threshold) demonstrates that short-duration, high-intensity outbursts (~13.7 mm/h over 5 hours) are equally capable of overcoming the soil's matric suction as prolonged, low-intensity soaking events (~0.15 mm/h over 8 days).

Figure 5 maps the normalised IMAP-D conditions, showing scaled intensities ranging from 1.31 x 10^{-4} to 0.012 h^{-1}. Normalisation effectively constrained regional variances, tightening the clustering of data points.

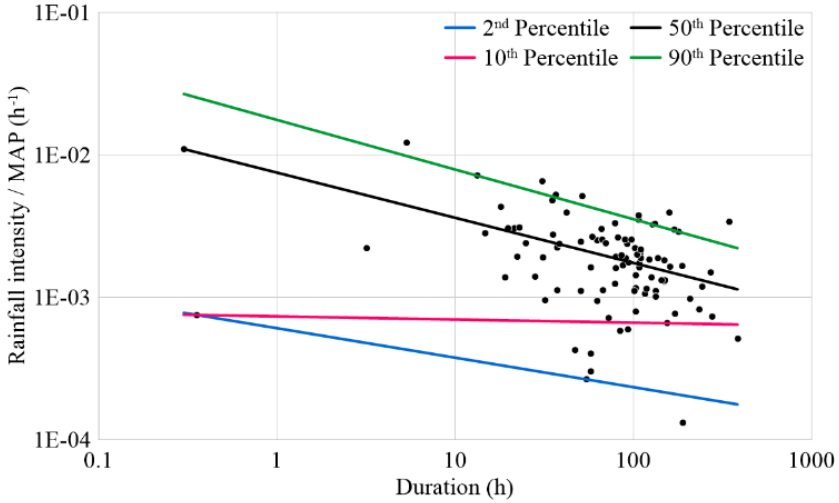

Figure 5. Rainfall IMAP-D conditions for shallow landslides in SEQ and the quantile regression lines for 2nd, 10th, 50th and 90th percentiles.

The rescaled model results are presented in Tables 3 and 4.

Table 3. Linearised IMAP-D thresholds for landslides initiation in SEQ.

 doi:10.20944/preprints202604.0798.v1

Quantile	IMAP-D threshold equation
2nd	$\log I_{MAP} = -0.20713 \log D + (-3.21683)$
10th	$\log I_{MAP} = -0.02215 \log D + (-3.13366)$
50th	$\log I_{MAP} = -0.31719 \log D + (-2.12413)$
90th	$\log I_{MAP} = -0.34876 \log D + (-1.75387)$

Table 4. IMAP-D threshold equations for SEQ.

Quantile	IMAP-D threshold equation	Duration range (h)
2nd	$I_{MAP} = 6.070 \times 10^{-4} D^{-0.20713}$	$0.3 \leq D \leq 383$
10th	$I_{MAP} = 7.351 \times 10^{-4} D^{-0.02215}$	$0.3 \leq D \leq 383$
50th	$I_{MAP} = 7.514 \times 10^{-3} D^{-0.31719}$	$0.3 \leq D \leq 383$
90th	$I_{MAP} = 1.763 \times 10^{-2} D^{-0.34876}$	$0.3 \leq D \leq 383$

As in rainfall I-D thresholds, considering the 50th percentile regression line, the general trend is that with the increase in rainfall duration, the IMAP decreases. The same trend is followed by the other IMAP-D regression lines as well, ranging the exponent (c) from (-0.222) to (-0.349). Moreover, the IMAP threshold depicts that the rescaled rainfall intensities of 5.22 x 10-5 h^{-1} have the potential of initiating a shallow slope failure.

6. Discussion

Contextualising the SEQ findings requires comparing them against established global and regional thresholds, detailed in Tables 5 and 6 and visualised in Figures 6 and 7.

Table 5. Existing I-D thresholds.

Reference	Equation	Duration range (h)
Caine (1980) [9]	$I = 14.82\ D^{-0.39}$	$0.167 < D < 500$
	$I = 2.20\ D^{-0.44}$	$0.1 < D < 1000$
Guzzetti et al. (2008) [4]	$I = 2.28\ D^{-0.20}$	$0.1 < D < 48$
	$I = 0.48\ D^{-0.11}$	$48 \leq D < 1000$
Saito et al. (2010) [10]	$I = 2.18\ D^{-0.26}$	$3 < D < 537$
Ravindran et al. (2019) [7]	$I = 22.6\ D^{-0.554}$	$48 < D < 432$

Note – [9] and [4] present global thresholds. [10] and [7] presented the regional thresholds for Japan and Northern New South Wales (NSW), respectively.

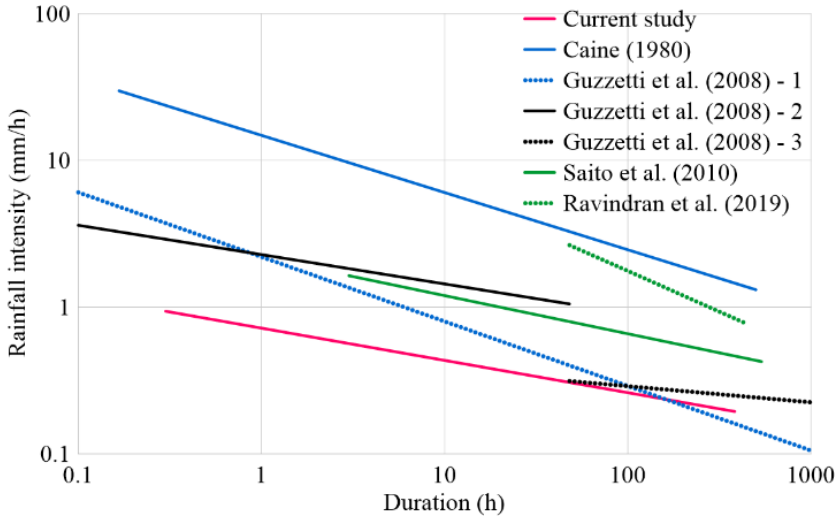

Figure 6. Comparison of Rainfall I-D conditions for shallow landslides in SEQ with existing thresholds.

 doi:10.20944/preprints202604.0798.v1

Table 6. Existing I_{MAP}-D thresholds.

Reference	Equation	Duration range (h)
Jibson (1989) [20]	$I_{MAP} = 0.02\ D^{-0.65}$	$0.5 < D < 12$
	$I_{MAP} = 0.0016\ D^{-0.40}$	$0.1 < D < 1000$
Guzzetti et al. (2008) [4]	$I_{MAP} = 0.0017\ D^{-0.13}$	$0.1 < D < 48$
	$I_{MAP} = 0.0005\ D^{-0.13}$	$48 \leq D < 1000$
Saito et al. (2010) [10]	$I_{MAP} = 0.0007\ D^{-0.21}$	$3 < D < 537$

Note – [20] and [4] presented global thresholds. [10] presented the regional thresholds for Japan.

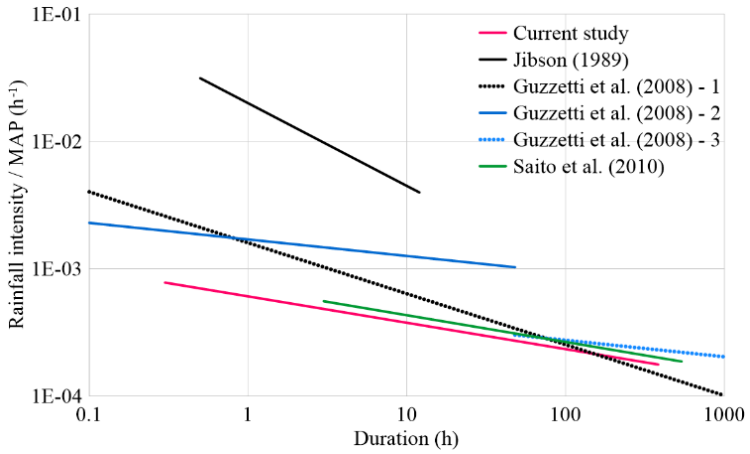

Figure 7. Comparison of Rainfall I_{MAP}-D conditions for shallow landslides in SEQ with existing thresholds.

The analysis clearly indicates that the mathematically derived I-D and I_{MAP}-D thresholds for SEQ sit considerably lower than both standard global metrics and the regionally proximal northern NSW threshold. This downward shift in the trigger boundary is particularly pronounced during short-duration storms (i.e., < 100 h). The expansive nature of the dataset, which captured numerous small-scale, highly localised failures often missed by generalised studies, provides a more granular understanding of regional soil sensitivity.

Interestingly, the normalised threshold (I_{MAP}-D) generated for Japan [10] traces a trajectory closely aligned with the new SEQ model. This suggests that the shared humid subtropical climatic settings, combined with structurally similar highly weathered residual soil profiles, dictate similar hydro-geomechanical failure mechanisms regardless of geographic separation.

Conversely, despite geographic proximity, the northern NSW threshold ($I = 22.6\ D^{-0.554}$) [7] is radically higher than the comparable SEQ 50th percentile threshold ($I = 5.83\ D^{-0.208}$). This underscores the danger of extrapolating empirical thresholds across state boundaries. Differing sample sizes (104 events in SEQ vs. a significantly smaller sample in NSW) and localised variations in stratigraphy necessitate dedicated, strictly localised threshold models.

To physically validate the empirical model, the calculated I-D threshold was superimposed against highly accurate, real-time geomechanical data from an active slope monitoring network located in Maleny, Queensland. These critical slopes utilise a telemetry network of Micro-Electro-Mechanical Systems (MEMS) tilt sensors and volumetric water content probes integrated with an on-site data transmission unit (DTU) [21]. Data polled every 10 minutes confirms active kinematic rotation and localised pore water trends. Five (5) separate kinematic failure events confirmed via this system between 2016 and 2020, all successfully plotted above the newly established SEQ 2nd percentile threshold (Figure 8). This ground-truthing exercise confirms the model's accuracy, eliminating theoretical false positives while successfully capturing all known true-positive failures.

 doi:10.20944/preprints202604.0798.v1

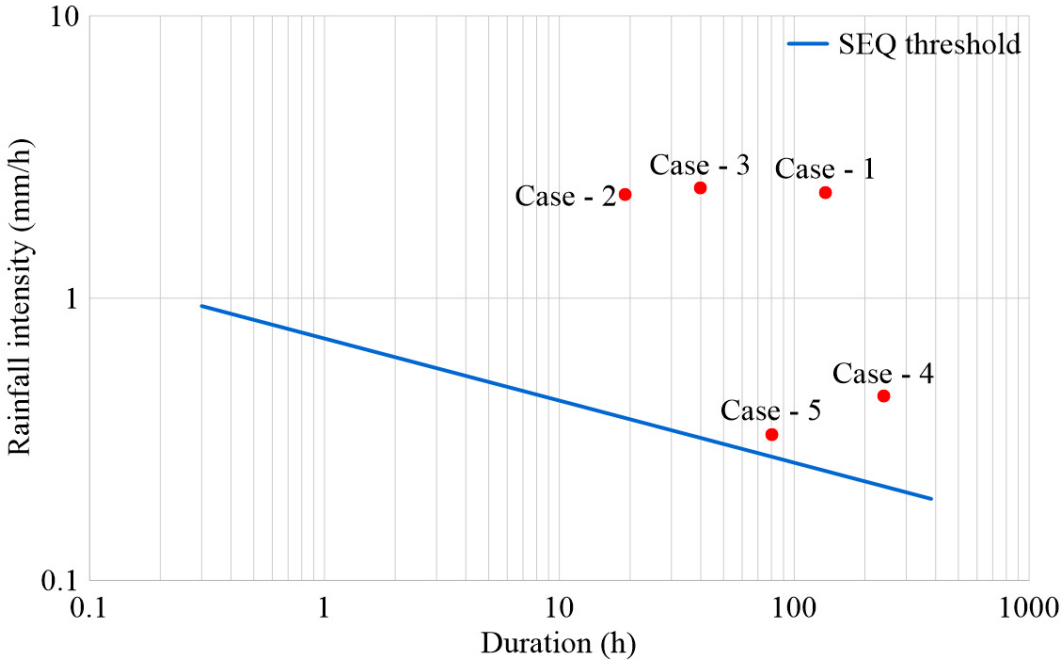

Figure 8. Validation of the applicability of the SEQ rainfall I-D threshold equation using real-time monitoring data.

It must be noted that methodological variations, such as reliance on interpolated rather than localised pluviographic data, inject some degree of uncertainty. Australia's vast landmass means that despite over 18,000 national weather stations, proximal data is often unavailable for discrete geological failures, resulting in the necessary exclusion of multiple historical events. Enhancing the resolution of spatial rainfall tracking remains a priority for refining future threshold models.

7. Conclusions

This study successfully formulated robust empirical I-D and normalised I_{MAP}-D thresholds for initiating shallow landslides in South-East Queensland. By leveraging quantile regression methodologies against a heavily vetted dataset of 104 localised slope failures (from an initial pool of 156), the study provides statistically resistant boundaries against historical outliers.

The resulting parameters reveal a high degree of regional susceptibility; rainfall intensities as low as 0.15 mm/h over extended durations are capable of initiating slope instability. These new regional thresholds are notably lower than corresponding global limits, capturing the specific geomechanical vulnerabilities of SEQ driven by intense summer precipitation patterns and significant topographic relief.

Author Contributions: Conceptualisation, Chaminda Gallage and Tharindu Abeykoon; methodology, Chaminda Gallage; software, Chaminda Gallage and Tharindu Abeykoon; validation, Chaminda Gallage and Tharindu Abeykoon; formal analysis, Chaminda Gallage; investigation, Chaminda Gallage; resources, Chaminda Gallage; data curation, Chaminda Gallage; writing - original draft preparation, Tharindu Abeykoon; writing - review and editing, Chaminda Gallage and Jessica Trofimovs; visualisation, Tharindu Abeykoon; supervision, Chaminda Gallage and Jessica Trofimovs; project administration, Chaminda Gallage and Jessica Trofimovs; funding acquisition, Chaminda Gallage and Jessica Trofimovs. All authors have read and agreed to the published version of the manuscript.

Funding: This research received no external funding.

Data Availability Statement: The data presented in this study are available on request from the corresponding author due to access restriction as the original dataset forms part of, Developing an economical and reliable real-

 doi:10.20944/preprints202604.0798.v1

time warning system for rainfall-induced individual landslides, Ph.D. Thesis, Queensland University of Technology, Brisbane, Australia, January 2022.

Acknowledgments: Authors gratefully acknowledge the BOM, Australia, especially Mr Lesley Rowland from Climate Data Services, for his kind support in providing the required rainfall data for the study. Further, gratitude should be extended to Geoscience Australia for maintaining the landslide database of Australia. The second author acknowledges the scholarship for the doctoral degree received from QUT, Australia.

Conflicts of Interest: The authors declare no conflict of interest. The authors declare that this study received in-kind support from BOM and Geoscience Australia. BOM and Geoscience Australia were not involved in the study design, collection, analysis, interpretation of data, the writing of this article or the decision to submit it for publication.

List of Notations

BOM	Bureau of Meteorology
MAP	Mean Annual Precipitation
SEQ	South East Queensland
I-D	Intensity - Duration
IDW	Inverse Distance Weighting
E-D	Event rainfall - Duration
DEM	Digital Elevation Model
GIS	Geographic Information System

References

1. Keefer, D. K.; Wilson, R. C.; Mark, R. K.; Brabb, E. E.; Brown, W. M.; Ellen, S. D.; Harp, E. L.; Wieczorek, G. F.; Alger, C. S.; Zatkin, R. S. Real-time landslide warning during heavy rainfall. *Science* **1987**, *238*(4829), 921-925.
2. Aleotti, P. A warning system for rainfall-induced shallow failures. *Engineering Geology* **2004**, *73*(3), 247-265.
3. Baum, R. L.; Godt, J. W.; Savage, W. Z. Estimating the timing and location of shallow rainfall-induced landslides using a model for transient, unsaturated infiltration. Journal of Geophysical Research. Earth Surface **2010**, *115*(3).
4. Guzzetti, F.; Peruccacci, S.; Rossi, M.; Stark, C. P. The rainfall intensity-duration control of shallow landslides and debris flows: an update. *Landslides* **2008**, *5*(1), 3-17.
5. Guzzetti, F.; Peruccacci, S.; Rossi, M.; Stark, C. P. Rainfall thresholds for the initiation of landslides in central and southern Europe. *Meteorology and Atmospheric Physics* **2007**, *98*(3), 239-267.
6. Martelloni, et al. [Missing Full Reference Details - Please insert standard MDPI format here].
7. Ravindran, S.; Gratchev, I.; Jeng, D.-S. Analysis of rainfall-induced landslides in northern New South Wales, Australia. *Australian Geomechanics* **2019**, *54*(4), 85-99.
8. Abbot, J.; Marohasy, J. Application of artificial neural networks to rainfall forecasting in Queensland, Australia. *Advances in Atmospheric Sciences* **2012**, *29*(4), 717-730.
9. Caine, N. The Rainfall Intensity: Duration Control of Shallow Landslides and Debris Flows. Geografiska Annaler. Series A, Physical Geography **1980**, *62*(1/2), 23-27.
10. Saito, H.; Nakayama, D.; Matsuyama, H. Relationship between the initiation of a shallow landslide and rainfall intensity-duration thresholds in Japan. *Geomorphology* **2010**, *118*(1), 167-175.
11. Crosta, G. B.; Frattini, P. Rainfall thresholds for the triggering of soil slips and debris flows. *Proc. 2nd Plinius Conf. Mediterr. Storms, GNDCI, Perugia* **2001**, 463-488.
12. Jakob, M.; Weatherly, H. A hydroclimatic threshold for landslide initiation on the North Shore Mountains of Vancouver, British Columbia. *Geomorphology* **2003**, *54*(3-4), 137-156.
13. Cannon, S. H. Regional rainfall-threshold conditions for abundant debris-flow activity. In *Landslides, Floods, and Marine Effects of the Storm of January 3-5, 1982, in the San Francisco Bay Region, California*; U.S. Geological Survey Professional Paper 1434; **1988**, 35-42.
14. Queensland Government. *South East Queensland Regional Plan*. Queensland Government, Brisbane, Australia, **2020**.

 doi:10.20944/preprints202604.0798.v1

15. Arifin, Z.; Ibrahim, M. R.; Hatta, H. R. Nearest tourism site searching using Haversine method. *Proc., 2016 3rd International Conference on Information Technology, Computer, and Electrical Engineering (ICITACEE)*, IEEE, **2016**, 293-296.
16. Winarno, E.; Hadikurniawati, W.; Rosso, R. N. Location based service for presence system using haversine method. *Proc., 2017 International Conference on Innovative and Creative Information Technology (ICITech)*, IEEE, **2017**, 1-4.
17. Lu, G. Y.; Wong, D. W. An adaptive inverse-distance weighting spatial interpolation technique. *Computers & Geosciences* **2008**, *34*(9), 1044-1055.
18. Koenker, R.; Hallock, K. F. Quantile regression. *Journal of economic perspectives* **2001**, *15*(4), 143-156.
19. Ford, C. Getting Started with Quantile Regression. *Statistical Research Consultant*, Research Data Services, **2015**.
20. Jibson, R. W. Debris flows in southern Puerto Rico. Landslide processes of the eastern United States and Puerto Rico, Geological Society of America special paper **1989**, 236, 29-55.
21. Abeykoon, T.; Gallage, C.; Dareeju, B.; Trofimovs, J. Real-time monitoring and wireless data transmission to predict rain-induced landslides in critical slopes. *Australian Geomechanics Journal* **2018**, *53*, 61-76.